ЯФ, 1966, т. 4, №3, с. 567-577.

ОБЪЕДИНЕННЫЙ
ИНСТИТУТ
ЯДЕРНЫХ
ИССЛЕДОВАНИЙ

Дубна

Е - 2560

Z. Janout, Yu.M. Kazarinov, F. Lehar,
A.F. Pisarev, Yu.N. Simonov

MEASUREMENT OF THE PARAMETER R IN THE ELASTIC pn- SCATTERING AT 605 MEV AND THE NUCLEON-NUCLEON PHASE SHIFT ANALYSIS

1966

E - 2560

Z. Janout, Yu.M. Kazarinov, F. Lehar,
A.F. Pisarev, Yu.N. Simonov

MEASUREMENT OF THE PARAMETER R IN THE ELASTIC pn- SCATTERING AT 605 MEV AND THE NUCLEON-NUCLEON PHASE SHIFT ANALYSIS

Submitted to JNP

In papers on the phase shift analysis it has been shown that existing experimental data make it possible to determine the nucleon-nucleon scattering amplitude uniquely in the 50-310 MeV energy region. The situation is quite different above the threshold of meson production. The phase shift analysis[1] has given three sets of phase shifts having approximately equal probabilities. The dependence of experimental data on the scattering angle given in ref.[1] for all three sets of phase shifts indicates that the simplest way to determine the scattering amplitude uniquely in this case is to measure the triple np-scattering parameters[2]. The planning of the experiment[3] has shown that the best angles at which to measure the parameters R_{pn} so as to determine the most probable phase shift set with minimal time loss are $\theta_2 = 70^\circ$, 90° and 125° (c.m.s.). In this paper we give the first results on R_{pn} measurements at 605 MeV[x].

INTRODUCTION

In order to determine the parameter R as well as any other Wolfenstein[2] parameter it is necessary to scatter a beam on three targets successively. Thus, the first scattering is used to obtain a beam with the polarization $\vec{P}_1$. The second scattering is the process in which the investigated rotation of the polarization vector occurs. The spin state after the second scattering is determined in the third analyzing scattering.

The general expression for the polarization $\langle \vec{\sigma} \rangle_2$ of an initially polarized beam with the polarization $\vec{P}_1$ scattered on an unpolarized target with spin 1/2 is

---

x/ The preliminary results of R_{pn} measurements at 90° were reported at the XII International Conference on High Energy Physics in Dubna, 1964.

$$I_2 \langle \vec{\sigma} \rangle_2 = I_2^0 \{[P_2 + D(\vec{P}_1, \vec{n}_2)]\vec{n}_2 +$$

$$+[A(\vec{P}_1, \vec{k}_2) + R(\vec{P}_1, \vec{n}_2 \times \vec{k}_2)]\vec{s}_2 \times +$$

$$+[A'(\vec{P}_1, \vec{k}_2) + R'(\vec{P}_1, \vec{n}_2 \times \vec{k}_2)]\vec{k}'_2 , \qquad (1)$$

where $I_2 = I_2^0 (1 + \vec{P}_1 \vec{P}_2)$, $\vec{n}_1$ and $\vec{n}_2$ are unit vectors normal to the first and second scattering planes, P_2 is polarization in the scattering of the unpolarized beam. D, R, A, R' , A' are Wolfenstein parameters.

$$\vec{s}_2 = \vec{n}_2 \times \vec{k}_2 \; ; \; (\vec{n}_1, \vec{n}_2) = \cos\phi_2 \; ; \; (\vec{n}_1, \vec{n}_2 \times \vec{k}_2) = \sin\phi_2$$

$\vec{k}_2$, $\vec{k}'_2$ are unit vectors in the direction of the particle momenta before and after the second scattering. Taking directions of $\vec{n}_1$ and $\vec{n}_2$, we obtain expressions (1) for $I_2 \langle \vec{\sigma} \rangle_2$ depending only on one or two Wolfenstein parameters. For example, considering the case $\vec{n}_1 \perp \vec{n}_2$ we find

$$I_2 \langle \vec{\sigma} \rangle_2 = I_2^0 \{P_2 \vec{n}_2 + RP_1 \vec{s}_2 + R'P_1 \vec{k}'_2\} . \qquad (2)$$

In this case the angular distribution of the scattered particles after the third scattering is

$$\overset{\downarrow}{I}_3 = I_3^0 \{1 + P_3 [P_2 \cos\phi_3 - RP_1 \sin\phi_3]\} \qquad (3)$$

$$(\vec{s}_2, \vec{n}_3) = (\vec{n}_2 \times \vec{k}_2, \vec{n}_3) = -\sin\phi_3$$

$$(\vec{n}_2, \vec{n}_3) = \cos\phi_3 .$$

Expression (3) indicates the possible ways of determining R. First of all it is the measurement of the "up-down" asymmetry ϵ_3 in the third scattering connected with R by the relation: $\epsilon_3 = -RP_1 P_3$. This method was previously used to determine R in pp-scattering. However, in view of the low intensity of polarized beams and low efficiency of neutron detectors, this method in the case of pn-scattering, involves great experimental difficulties. The measurement of triple pn-scattering parameters is possible only using a detector with a large solid angle in the third scattering. The simplest possibility is probably io use a spark chamber as a detector.

Working with spark chambers it is better to determine the parameter R by the maximum likelihood method [4] since we use the angular distribution in the whole interval of the scattering angles θ_3 and ϕ_3 (lab. syst.). Besides, P_2 may be simultaneously determined using the same experimental data.

When n particles are scattered at the angles θ_3^i and ϕ_3^i the likelihood function has the following form:

$$L(P_2, R) = \prod_{i=1}^{n} [1 + P_3(\theta_3^i)(P_2 \cos\phi_3^i - RP_1 \sin\phi_3^i)] . \qquad (4)$$

The most probable values of P_2 and R are determined from the condition that the likelihood function should have a maximum. The method of determining this maximum as well as the errors of the considered values P_2 and R is treated in detail in ref. [5] .

It should be noted that expression (3) can be used to find ways of excluding experimental errors in the determination of P_2 and R, due to imperfections in the measuring equipment. The corresponding values of the instrumental" parameters can be determined using an unpolarized beam($\langle \vec{\sigma} \rangle_2 = 0$) in the third scattering. These errors in determining R may also be excluded if the measurement is carried out with the change of the polarization direction P_1. For $\vec{P}_1$ parallel or antiparallel to the vector $\vec{n}_2 \times \vec{k}_2$, respectively, expression (3) reduces to

$$I_3 = I_3^0 \{1 + P_3 (P_2 \cos\phi_3 \mp RP_1 \sin\phi_3)\} . \qquad (5)$$

Since the sign of the "instrumental" value R^I does not change when the direction of $\vec{P}_1$ is reversed, the mean values of R for the primary beam polarizations $\vec{P}_1$ and $-\vec{P}_1$ will be equal to the real value of R.

EXPERIMENTAL EQUIPMENT

The scheme of the R_{pn} experiment for $\theta_2 = 90^\circ$ and 125° is given in Fig. 1. The polarized particle beam was produced by scattering the external proton beam from the accelerator 1 on carbon target 5. The external proton beam was deflected 2° upwards with the help of the magnet pole pieces 2 placed in the fringing magnetic field of the accelerator and was focused by quadrupole magnetic lenses 3. After being deviated 8° downwards with the help of the auxiliary magnet 4 the beam was scattered on the carbon target. The thickness of the target was $23\,g/cm^2$. Protons scattered on carbon 6° upwards produced the resulting beam with the polarization $P_1 = 0.37 \pm 0.03$.

In order to exclude the "instrumental" effects in the measurements at $\theta_2 = 125^\circ$ (c.m.s.) the direction of the polarization vector $\vec{P}_1$ was changed to the opposite one during the experiment. The change in the arrangement of the equipment shaping the polarized beam in this case is shown by the dashed line in Fig. 1. The unpolarized 605 MeV proton beam was used for the same reason in the experiment at $\theta_2 = 90^\circ$.

The polarized proton beam was focused by quadrupole magnetic lenses 7 passed through a collimator in the screening wall of the accelerator 8 and was deviated by the magnet 9 by 6° upwards. This also served to separate from the beam the admixture of neutral particles mainly neutrons produced by the charge exchange scattering of protons on carbon. Since the vector of the magnetic field strength is parallel (or antiparallel) to the polarization vector $\vec{P}_1$ during the deviation of the beam, the polarization $\vec{P}_1$ is not changed. Having passed through additional collimators the polarized beam hit the "neutron" target and was scattered for the second time. The beam intensity was 2.10^6 protons/cm^2 sec at 605 ± 9 MeV [12] at the point of the second scattering.

Neutrons in deuterons were used as a "neutron" target. The CD_2-C difference was measured; quasielastic pp-scattering was excluded by an anticoincidence counter. Heavy polyethylene (5.28 g/cm^2) and graphite (4.07 g/cm^2) cylinders were used as scatterers in the measurement at 90°; at 125° the thickness of scatterers was 4.3 g/cm^2 and 3.26 g/cm^2 for CD_2 and C, respectively. Hydrogen atoms were replaced by deuterium ones in heavy polyethylene by 98%. The angular resolution in the second scattering was $\Delta\theta_2 = \pm 1.4^\circ$.

The block-diagram of the electronic part of the equipment is shown in Fig. 2. C_1, C_2 and C_5 were conventional scintillation counters. The counters C_3 and C_4 were neutron detectors [6] and detected "stars" produced in the nuclear interactions of neutrons in the scintillators of these counters. The detection efficiency of the counters for charged relativistic particles was much decreased by the choice of a correct photomultiplier regime, detection efficiency for neutrons being completely maintained. The neutron detection efficiency of such a detector is rather low ($\approx 5\%$) and two neutron counters are used instead of one, so as to increase the counting rate.

Elastic scattering events on neutrons in deuterium were detected by a telescope consisting of the scintillation counters C_1 and C_2 connected in coincidence with the neutron counter C_3 or C_4. The counter C_5 connected in anticoincidence with other counters was used to remove the background of charged particles, mainly due to the quasielastic pp-collisions. A coincidence circuit with

distributed amplification described in ref. [7] was employed in the measurements. The resolution time of the coincidence circuit was chosen to be equal to 10 nsec. A pulse from the output of the coincidence circuit triggered the pulse generators feeding spark chambers, picture counting and camera control circuits.

The polarization $\langle\vec{\sigma}\rangle_2$ in the second scattering was analyzed by scattering on an analyzing target placed inside the spark chamber 19 (Fig. 1). Aluminium (24 g/cm^2) and carbon (6.75 g/cm^2) analyzers were used at 90° and 125°, respectively. In both cases the target was divided into two parts to decrease the multiple Coulomb scattering. Aluminium was used because its analyzing power was determined previously [8]. Carbon was chosen in view of the necessity to decrease the mean angle of the multiple Coulomb scattering.

The spark chamber 15 made it possible to exclude reliably events in which a charged particle passes through the neutron counter. The projection of tracks in chambers on two interperpendicular planes was photographed using a standard 35 mm film. The whole experimental equipment was protected by a lead screening.

Measurement

The angular distribution of protons scattered on the analyzer was observed when a CD_2 ($I_3^{CD_2}$) target was put into the beam as the second scatterer. The p, n-scattering occurred in this case either on the deuterium neutrons or on neutrons bound in carbon nuclei. The second effect is the background. It was determined by observing the proton angular distribution I_3^C in the chamber when the CD_2 scatterer was replaced by a carbon (C) scatterer[x]. The ratio of CD_2 and C effects was 1:3 and 1:4 for angles of 90° and 125°, respectively.

It should be noted that the chamber background was increased several times due to the relatively long time of the spark chamber "memory" (about 1 μ sec). The long "memory" time sometimes caused the appearence of pictures with two or more particle tracks. Since pictures with more than one track were not treated, such a background was excluded in scanning.

One of the most important stages of the experiment were the following: the determination of "instrumental" parameters and the measurement of the ana-

---

x/ If anticoincidences were insufficient, the background could also be caused by the scattering of protons on protons contained in deuterium and carbon nuclei. However, additional experiments determining the difference between effects on CH_2 and CD_2 targets equivalent with respect to the number of nuclei have shown that this background is negligible.

lyzing power P_3 in the third scattering. The analyzing power was taken from ref.[8] in experiments at 90°. The "instrumental" parameters were measured using an unpolarized proton beam. The anisotropy I_3 of the angular distribution I_3^I (with respect to the azimuthal angle) in this case is due completely to the imperfections of the experimental arrangement. It was used to correct the results of the measurements. The "instrumental" parameters were not determined at the angle of 125°. Since the measurement of R was carried out for two opposite directions of the primary beam polarization P_1 the "instrumental" effects were excluded. The real value of R was obtained by averaging the two measured values.

For P_3 measurements at an angle $\theta_2 = 125^\circ$ a spark chamber with the analyzers (graphite blocks) inside it was placed into the polarized 135 MeV proton beam (the energy of protons after the second scattering at the angle $\theta_2 = 125^\circ$). To obtain this energy the 605 MeV polarized proton beam with the polarization $P_1 = 0.37 \pm 0.03$ was passed through a polyethylene absorber. The P_3 measurements as well as the main experiments were performed for two directions of P_1.

Treatment of Experimental Data and Results

The number of useful events is shown in Table 1

Table 1

Scatterer in the second scattering	Angle of the second scattering	Number of events	Note
CD_2	90°	5671	Main experiments
C	90°	2962	
H_2	90°	15836	"Instrumental" parameters measured with an unpolarized beam
CD_2	125°	5630	Main experiment
C	125°	797	
-	-	9355	Determination of P_3 at 135 MeV
		40251	Total number of events

Data on preliminary experiments at 90° were treated using a diascope. The main information was treated with a semi-automatic device specially developed

for these purposes[9]. The results were written down by the device in Grey code on five-track paper punched tape which was then treated on an electronic computer[10]. Corrections for geometrical distortions arising in taking track pictures[11] were introduced in the treatment.

Useful events were selected in the scanning of pictures according to the following criteria:

1. A picture has only one track in the proton branch.

2. There is no track in the neutron branch in the corresponding picture.

3. The deflection angle of the proton track in the chamber exceeds 2° at least in one projection.

Additional requirements were imposed in the treatment on the computer.

1. The third scattering angle θ_3 should lie within $4^\circ \leq \theta_3 \leq 30^\circ$.

2. The angle at which the track enters into the spark chamber differed from the mean entrance angle determined from a large number of events by no more than 3°.

The lower limit of the scattering angle θ_3 was determined so that the effective cross section of the Coulomb scattering was smaller than that of nuclear scattering. The upper limit is due to the fact that above 30° the effective cross section decreases, the contribution of inelastic collisions increases and the analyzing power is reduced.

For the treatment on an electronic computer the angular distribution of protons in the spark chamber (in all the cases) is approximated by expression (3):

$$I_3(\theta_3, \phi_3) = I_3^0(\theta_3)\{1 + P_3(\theta_3)[P_2 \cos\phi_3 - PP_1 \sin\phi_3]\}.$$

The most probable values of the unknown parameters P_2 and R were found from the condition of the maximum likelihood function[4]. The maximum was obtained by the linearization method which allows simultaneously to find the most probable parameter values and to determine their errors taking into account the errors of other quantities in (3), refs.[5,10].

When P_2 and R were determined for 90° we proceeded from the fact that the angular distribution I_3^{pn} of protons after pn-collision in the second scattering can be expressed in terms of the experimentally measured angular distribution $I_3^{CD_2}$, I_3^C and I_3^I

$$I_3^{pn} = (I_3^{CD_2} - K_2 I_3^{C} - K_1 I_3^{I}) \frac{1}{K_1} ,$$

where K_1 and K_2 are relative probabilities for scattering on D_2 and C contained in a CD_2 scatterer, respectively, normalized so that $K_1 + K_2 = 1$. Using (3) and (6) one can easily obtain

$$P_2 = (P_2^{CD_2} - K_2 P_2^{C} - K_1 P_2^{I}) \cdot \frac{1}{K_1} ,$$
$$R = (R^{CD_2} - K_2 R^{C} - K_1 R^{I}) \cdot \frac{1}{K_1} , \qquad (7)$$

where $P_2^{CD_2}$, P_2^{C} , R^{CD_2} , R^{C} , P_2^{I} and R^{I} are parameters obtained in treating the corresponding angular distributions.

The relative probabilities of scattering on K_1 and K_2 were determined experimentally from the corresponding counting rates. For the angle $\theta_2 = 90^\circ$ these values are $K_1 = 0.699$ and $K_2 = 0.301$.

As has already been mentioned, in experiments at an angle of 125° "instrumental" effects in the proton angular distribution after the third scattering were excluded by averaging the results obtained at two directions of the primary beam polarization $\vec{P}_1$. In this case P_2^{I} and R^{I} were set to be equal to zero in formulas (7). K_1 and K_2 for $\theta_2 = 125^\circ$ are 0.75 and 0.25, respectively. It is worth noting that the "instrumental" parameters $R^{I}(90^\circ)$ and $R^{I}(125^\circ)$ have been determined independtly of their source. This is seen from formula (3) since the change of P_1 directly affects the value of R. In the case of the polarization P_2 the correct value of P_2 was found only in measurement at an angle of 90° when use was made of the unpolarized beam (the angle of scattering for $\theta_2 = 90^\circ$ was established to an accuracy of $\pm 12'$). In rotating the polarization vector $\vec{P}_1$ by 180° only a part of the "instrumental" effects in P_2 was excluded connected directly with the beam (e.g., non-perpendicularity of the planes of the first and second scatterings). Estimations showed that the change of the polarization P_2 due to the mentioned effect can be at most ± 0.014.

Table 2 presents for comparison the values $P_2^{I}\,\overline{P_3(\theta_3)} = \epsilon_P$ and $P_1 R^{I}\,\overline{P_3(\theta_3)} = \epsilon_R$ for measurements at the angles 90° and 125°. These are the averaged right-left and up-down scattering asymmetries, respectively.

In this case

$$\overline{P_3(\theta_3)} = \frac{\int_{\theta_{3min}}^{\theta_{3max}} P_3(\theta_3) \cdot I_3^0 \, d\theta_3}{\int_{\theta_{3min}}^{\theta_{3max}} I_3^0 \, d\theta_3} ,$$

where I_3^0 is the effective cross section for the scattering of unpolarized protons on the analyzer.

Table 2

	$\theta_{3min} - \theta_{3max}$	$\epsilon_P \pm \Delta\epsilon_P$	$\epsilon_R \pm \Delta\epsilon_R$
90°	$6^\circ - 30^\circ$	0.0685 ± 0.009	0.055 ± 0.006
	$7^\circ - 30^\circ$	0.049 ± 0.010	0.039 ± 0.006
125°	$6^\circ - 30^\circ$	0.026 ± 0.026	0.084 ± 0.016
	$7^\circ - 30^\circ$	0.013 ± 0.030	0.057 ± 0.017

It is seen from Table 2 that ϵ_P and ϵ_R in both cases coincide within errors.

In treating the results the smallest value for the angle θ_3 was determined above which the Coulomb scattering ceases to be important. With this aim the data were treated in the range $\theta_{3min} \leq \theta_3 \leq 30^\circ$ and the values of θ_{3min} are taken from 4° to 12° (l.s.) with a 1° step. As a result it turned out that beginning from $\theta_{3min} = 6^\circ$ the values of the parameters P_2 and R are constant within the errors for all the treated angular distributions (Tables 3 and 4).

The value $P_1 = 0.37 \pm 0.03$ was taken from the renormalized results of ref.[12]. To determine the analyzing power $P_3(\theta_3)$ for Al in experiments at 90° the results of ref.[8] were used. Unfortunately, measurements of the analyzing power $P_3(\theta_3)$ for carbon at $\theta_2 = 125^\circ$ allow one to obtain only a rough estimate of $P_3(\theta_3)$ because of the short measuring time. The main source of information on P_3 was in this case ref.[13], in which polarization has been measured in 95 MeV proton scattering on carbon, was found taking into account inelastic collisions. In this case a normalizing factor taken from ref.[15] was introduced. The energy of 95 MeV approximately coincides with the main proton energy in the thrid scattering since the proton energy equal to 121 MeV at the chamber entrance is reduced to 72.5 MeV at the analyzer output.

Table 3

Results of treating experimental data in the interval $\theta_{3min} \le \theta_3 \le 30^\circ$ for various $\theta_{3\ min}$ with $\theta_2 = 90^\circ$

$\theta^\circ_{3\ min}$	P_2	$\pm\Delta P_2$	R	$\pm\Delta R$
4	0.060	0.061	0.256	0.115
5	-0.077	0.063	0.420	0.107
6	-0.070	0.064	0.500	0.107
7	-0.112	0.070	0.402	0.107
8	-0.105	0.074	0.360	0.107
9	-0.067	0.078	0.403	0.107
10	-0.009	0.084	0.451	0.108
11	0.035	0.087	0.546	0.110

Table 4

Results of treating experimental data in the interval $\theta_{3\ min} \le \theta_3 \le 30^\circ$ for various $\theta_{3\ min}$ with $\theta_2 = 125^\circ$

θ°_{3min}	P_2	$\pm\Delta P_2$	R	$\pm\Delta R$
4	-0.940	0.118	-0.146	0.201
5	-0.600	0.145	-0.167	0.239
6	-0.438	0.160	-0.059	0.258
7	-0.207	0.165	0.012	0.274
8	-0.154	0.174	-0.011	0.283
9	-0.039	0.185	-0.002	0.290
10	-0.074	0.193	0.021	0.298
11	-0.098	0.198	-0.053	0.302
12	-0.012	0.200	-0.052	0.309

The dependence $I_o P_3(\theta)$ on energy in our case is close to linear in a sufficiently wide energy range (Fig. 3). The averaged values $I_o P_3(\theta)$ in the energy interval from 72.5 to 121 MeV coincide within the errors with the value of $I_o P_3(\theta)$ at 95 MeV.

The dependence $P_3(\theta_3)$ was approximated by the function

$$P_3(\theta_3) = \sin\theta_3 \cdot \Sigma a_n \cos^n \theta_3 \qquad (8)$$

in treating the results. In all the cases the first four terms of series (8) described satisfactorily the experimental data.

CONCLUSION

The obtained values of the parameters

$$P_2(90^\circ) = -0.07 \pm 0.06 \qquad R(90^\circ) = 0.50 \pm 0.11$$
$$P_2(125^\circ) = -0.44 \pm 0.16 \qquad R(125^\circ) = -0.06 \pm 0.26$$

best of all agreed with the values calculated in ref.[1] using the second phase shift set, whereas the value of the parameter R excluded the first and third sets (the deviation was equal to six errors). However, it was known that a more detailed phase shift analysis in analogous conditions sometimes gives changed solutions which already describe the new data satisfactorily. In this connection the sets of phase shifts obtained earlier were specified using the new data on P_2 and R. It turned out that only the third solution (χ^2 is increased up to 143) is rejected, whereas the first and second ones remain approximately equally possible according to the χ^2 - criterion (χ^2 = 99.56 and 86.0, respectively). The new phase shifts of these sets are listed in Table 5.

Fig. 4 shows the angular dependence of the parameter R calculated from the two remaining phase shift sets. It is seen from the curves shown in Fig. 4, that the measurements of R with $\theta_2 = 60^\circ - 70^\circ$ are still the optimum way of determining the most probable of the two sets. Simultaneously with the determination of P_2 and R the same quantities have been measured in the quasielastic scattering of polarized protons on neutrons bound in carbon nuclei. The following results have been obtained:

$$P_2^c(90^\circ) = 0.02 \pm 0.06 \qquad R^c(90^\circ) = 0.23 \pm 0.11$$
$$P_2^c(125^\circ) = -0.27 \pm 0.26 \qquad R^c(125^\circ) = -0.49 \pm 0.41 .$$

It should be noted that the values of P_2 and R obtained in proton scattering on neutrons in deuterium nuclei can, in principle, differ from those for free p-n scattering. The corresponding corrections to experimental values have been calculated for the energy 147 MeV[16-21]. These calculations are not quite suitable for our case since they take into account only interactions in the S-

state. However, these corrections should decrease with decreasing angle and increasing energy and for our case they seem to be smaller than the experimental errors. Besides, direct experiments have shown that P_{pp} and D_{pp} in the case of elastic and quasi-elastic scattering (on a proton in a deutron) at 630 MeV coincide within experimental accuracy [22]. Nevertheless the problem of the problem of the corrections for quasielastic scattering deserves a special consideration.

In conclusion the authors wish to express their deep gratitude to S.M.Bilenky, J.Bystricky, V.P.Dzelepov, L.I.Lapidus, M.Maly, R.M.Ryndin, O.Shon, A.A.Tyapkin and P.Winternitz for valuable discussions and help in solving some of the problems; M.G.Mescheryakov and his group for information on the polarized proton beam and for granting the apparatus for extracting the beam; to B.Pavlickova for preparing capillary tubes of scintillating plastic for a neutron counter; to S.I.Bilenkaya, S.Belyakov, V.A.Maximova, V.M.Sakovsky, S.A.Smirnova, T.D.Timofeyeva for help; to V.V.Vishnyakov for valuable remarks and to A.M.Rozanova for participating in measurements at the angle of 90°. The authors are also grateful to the photolaboratory staff for developing a large amount of film.

Special thanks are to J.M.Dickson, B.Lowe and B.Rose for private communication.

References

1. Ю.М.Казаринов, В.С.Киселев. ЖЭТФ, 46, 789, 1964. Ю.М.Казаринов, В.С.Киселев, Ю.Н.Симонов. Препринт ОИЯИ Р-2241, 1965.
2. L.Wolfenstein. Phys. Rev., 96, 1654, 1954.
3. Ф.Легар, В.В.Федоров. Препринт ОИЯИ Р-2332, Дубна, 1965. Я.Ф. (в печати).
4. Д.Орир. Препринт ОИЯИ, R-292, Дубна, 1959 г.
5. И.Быстрицкий, Ф.Легар. Препринт ОИЯИ Р-2028, Дубна, 1965.
6. Ю.К.Акимов, А.С.Кузнецов, Г.А.Лексин. ПТЭ 2, 70, 1956.
7. Ю.М.Казаринов, Ю.Н.Симонов. Препринт ОИЯИ Р-1848, 1964.
8. Ю.М.Казаринов, Ф.Легар, Г. Петер, А.Ф. Писарев, К.М. Фальбрух. ЖЭТФ, 47, 9, 1964. Ю. Быстрицкий, Б.М. Головин, Р.Я. Зулькариеев, С.В. Медведь, В.И.Никаноров, А.Ф. Писарев. Труды конференции по физике высоких энергий. Дубна, 1964, стр. 14. Атомиздат.
9. Ф.Легар, М.Малы, О.Сгон. Препринт ОИЯИ Р-2340, Дубна 1965. ПТЭ (в печати).
10. И. Быстрицкий, Ф. Легар, П. Либл, М. Малы, О. Сгон, И. Фриш. Препринт ОИЯИ Р-2223, Дубна, 1965 г.

11. И. Быстрицкий, Ф. Легар, М. Малы, О. Сгон, З. Яноут. Препринт ОИЯИ Р-2420, Дубна, 1965.
12. Ю. П. Кумекин, М.Г. Мещеряков, С.Б. Нурушев, Г.Д. Столетов. ЖЭТФ 46, 50 (1964).
13. J.M.Dickson, D.C.Salter. Nuovo Cim., 6, 235, 1957.
14. H.P.Stapp, J.Y.Ypsilantis, N.Metropolis. Phys.Rev., 105, 302, 1957.
15. O.N.Jarvis, B.Rose. Phys.Lett., 15, 271, 1965.
16. J.Lefrancois, R.A.Hofman, E.H.Thorndike, R.Wilson. Phys. Rev., 131, 1660, 1963.
17. E.H.Thorndike, J.Lefrancois, R.Wilson. Phys.Rev., 120, 1819, 1960.
18. A.H.Cromer, E.H.Thorndike. Phys.Rev., 131, 1680, 1963.
19. A.H.Cromer. Phys.Rev., 129, 1672, 1963.
20. A.Everett. Phys.Rev., 126, 831, 1962.
21. P.F.Koehler, E.H.Thorndike, A.H.Cromer. Phys.Rev., 134 B, 1030, 1964.
22. Б.М.Головин, В.П.Джелепов, В.С.Надеждин, В.И.Сатаров. Труды XII Международной конференции по физике высоких энергий. Дубна, 1964 г. Атомиздат.
23. D.J.Steinberg, J.N.Palmieri, A.M.Cormac. Nucl. Phys., 56, 46, 1964.
24. O.N.Jarvis, G.F.Cox. Preprint AERE-R 5006 Harwell 1965.
25. O.N.Jarvis, B.Rose, J.P.Scanlon. Preprint AERE-4896. Harwell, 1965.
26. J.M.Dickson, D.C.Salter. Private Communication. Unpublished.

Received by Publishing Department
on February 1, 1965.

Table 5

Phase shifts	I-st set δ^0	I-st set $\pm\Delta\delta^0$	2-nd set δ^0	2-nd set $\pm\Delta\delta^0$
	Real parts of phase shifts			
f^2	0.088	0.008	0.063	0.009
$^1S_0$	-28.37	4.11	-24.95	2.53
$^3S_1$	- 3.13	9.16	2.26	7.51
$^3P_0$	-37.34	11.61	-50.94	14.53
$^1P_1$	-18.54	5.89	-60.37	9.45
$^3P_1$	-27.48	3.54	-35.83	4.46
$^3P_2$	27.53	2.52	20.93	1.63
ε_1	22.09	2.99	1.34	1.08
$^3D_1$	-15.38	3.75	18.52	1.07
$^1D_2$	7.43	1.73	6.00	2.51
$^3D_2$	17.61	3.55	21.96	5.93
$^3D_3$	- 1.11	3.57	9.91	4.13
ε_2	- 2.25	1.74	- 8.36	2.41
$^3F_2$	- 7.13	1.49	- 0.67	2.69
$^1F_3$	4.71	3.04	4.49	3.67
$^3F_3$	- 4.02	1.68	- 9.83	1.86
$^3F_4$	0.39	0.95	3.18	0.97
ε_3	18.83	0.97	1.40	7.64
$^3G_3$	- 1.15	2.76	3.13	4.05
$^1G_4$	6.13	0.75	5.96	0.74
$^3G_4$	2.29	2.58	- 3.37	2.92
$^3G_5$	- 2.47	2.02	0.82	1.35
ε_4	- 6.07	0.57	- 4.00	1.07
$^3H_4$	1.59	0.68	2.98	0.90
$^1H_5$	7.44	1.81	- 1.85	2.63
$^3H_5$	- 3.91	0.87	- 5.06	1.07
$^3H_6$	2.50	0.56	2.62	0.42
	Imaginary Parts of Phase Shifts			
$^3P_0$	2.13	5.18	5.38	7.38
$^3P_1$	- 3.17	2.30	-3.24	3.39
$^3P_2$	8.50	2.71	4.37	3.19
$^1D_2$	14.29	4.03	2.39	3.27
$^3F_2$	1.42	2.41	6.77	3.13
$^3F_3$	4.60	3.64	6.23	4.07
χ^2	99.64		85.81	

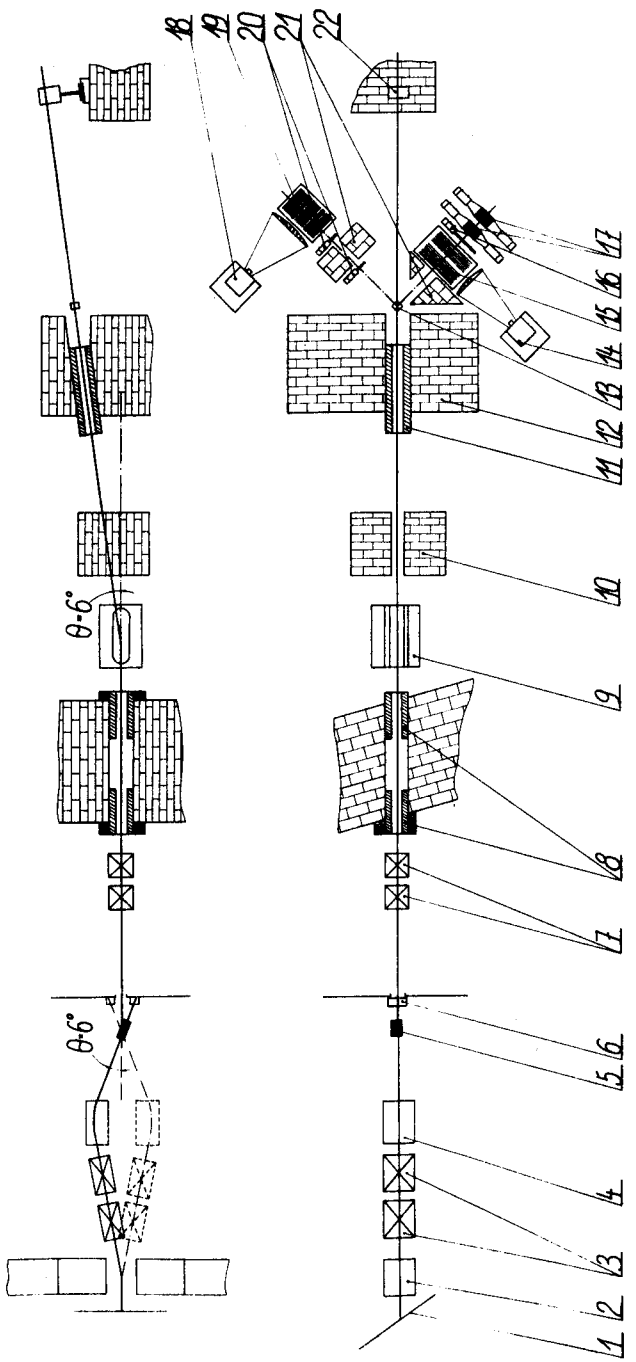

Fig. 1. Experimental equipment for the measurement of the parameter R in elastic pn scattering. 1 - window of the synchrocyclotron chamber, 2 - magnetic pole pieces; 3,7 - magnetic quadrupole lenses 4 - deflecting magnetic, 5 - first (carbon) scatterer, 6-monitor of the unpolarized beam, 8,11 - collimators, 9 - a separating magnet , 10,12,21- shielding, 13- the second target, 14,18- cameras, 15,19- spark chambers, 16- anticoincidence counter, 17- neutron detectors, 20- proton scintillation counters, 22- the monitor of the polarized proton beam.

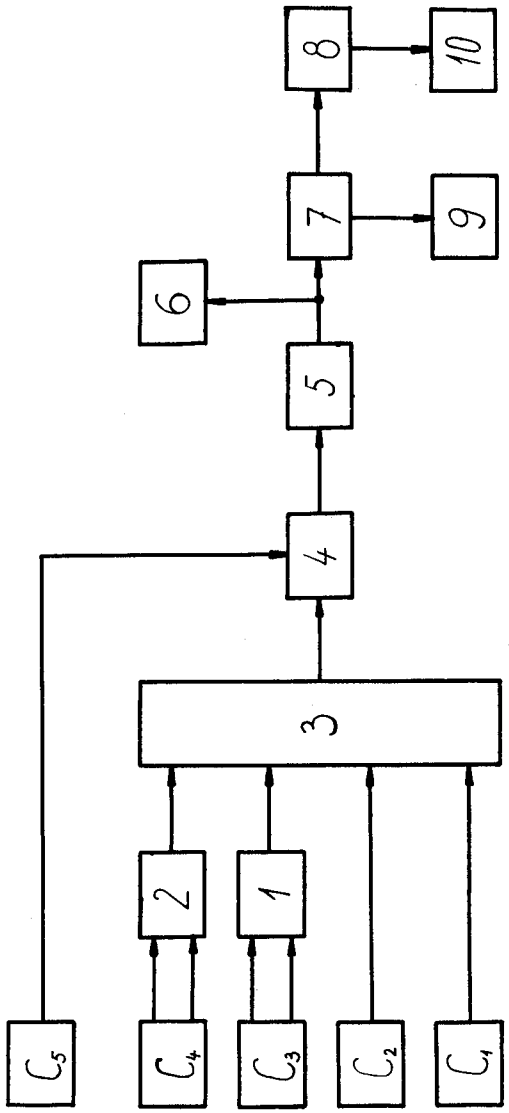

Fig. 2. Block-diagram of the electronic apparatus. C_1, C_2, C_5 - scintillation counters, C_3, C_4 - neutron counters, 1,2 - a pulse collecting circuit, 3 - a coincidence circuit, 4 - an anticoincidence circuit, 5 - an amplifier, 6 - a scaler, 7 - a pulse shaping circuit triggering the spark chambers, 8 - a circuit triggering cameras and picture indication, 9 - spark chambers, 10 - cameras.

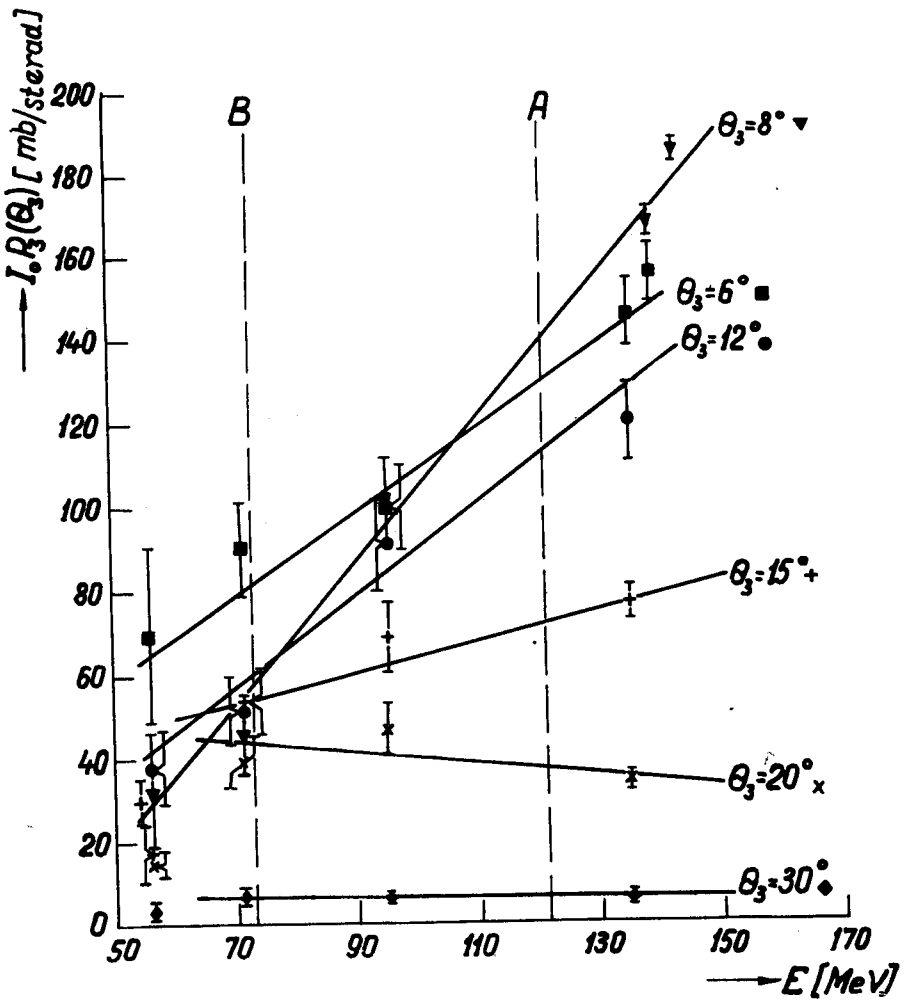

Fig. 3. Energy dependence of $I_0 P_3(\theta_3)$ for θ_3 = 6,8,12,15, 20, 30° (lab.system) calculated with the data of refs. / 13,15,23-26/. A - the energy of particles incident on the spark chamber, B - the energy of particles after the analyzer.

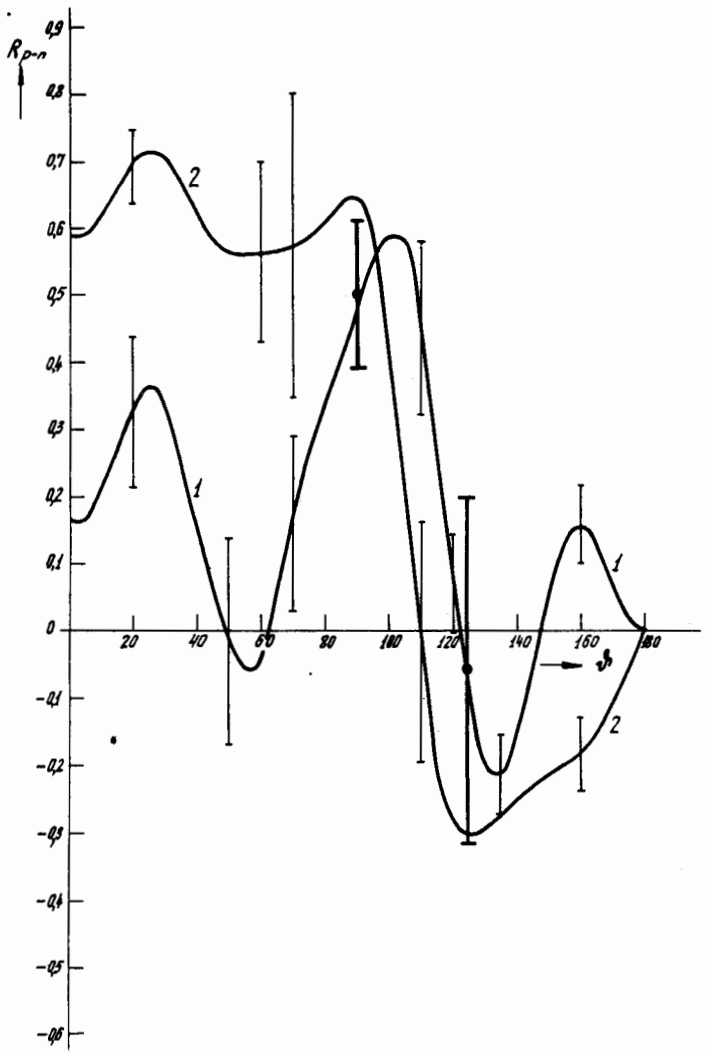

Fig. 4. Dependence of R_{pn} on the angle θ_2 (c.m.s.) calculated from the phase shift sets 1 and 2 in Table 5. The lines are the calculated corridor of errors, ⊕ - the experimental points measured in this investigation.